MOLECULAR AND CELLULAR BIOLOGY, May 2006, p. 3541–3549 Vol. 26, No. 9
0270-7306/06/$08.00+0 doi:10.1128/MCB.26.9.3541–3549.2006

The Murine Ortholog of *Notchless*, a Direct Regulator of the Notch Pathway in *Drosophila melanogaster*, Is Essential for Survival of Inner Cell Mass Cells

Sarah Cormier,[1]§ Stéphanie Le Bras,[1]†§ Céline Souilhol,[1] Sandrine Vandormael-Pournin,[1] Béatrice Durand,[2] Charles Babinet,[1]* Patricia Baldacci,[1]‡ and Michel Cohen-Tannoudji[1]

Unité Biologie du Développement, CNRS URA 2578, Institut Pasteur, Paris, France,[1] *and Unité des Rétrovirus et Transfert Génétiques, Institut Pasteur, Paris, France*[2]

Received 20 December 2005/Accepted 28 January 2006

Notch signaling is an evolutionarily conserved pathway involved in intercellular communication and is essential for proper cell fate choices. Numerous genes participate in the modulation of the Notch signaling pathway activity. Among them, Notchless (Nle) is a direct regulator of the Notch activity identified in *Drosophila melanogaster*. Here, we characterized the murine ortholog of Nle and demonstrated that it has conserved the ability to modulate Notch signaling. We also generated mice deficient for *mouse Nle* (*mNle*) and showed that its disruption resulted in embryonic lethality shortly after implantation. In late *mNle*$^{-/-}$ blastocysts, inner cell mass (ICM) cells died through a caspase 3-dependent apoptotic process. Most deficient embryos exhibited a delay in the temporal down-regulation of Oct4 expression in the trophectoderm (TE). However, *mNle*-deficient TE was able to induce decidual swelling in vivo and properly differentiated in vitro. Hence, our results indicate that *mNle* is mainly required in ICM cells, being instrumental for their survival, and raise the possibility that the death of *mNle*-deficient embryos might result from abnormal Notch signaling during the first steps of development.

The Notch signaling pathway plays a central role in the control of cell fate decisions in a wide variety of cell lineages during invertebrate and vertebrate development (1, 2, 24). Basically, this is achieved in two different ways, lateral inhibition and inductive signaling, to create either a group of highly similar cells or, in contrast, a mosaic of different cell types from a group of initially equivalent cells. Hence, the Notch signaling pathway is involved in the development of many cell types, and modification of its activity can dramatically affect proliferation, differentiation, and apoptotic events. The genes of the Notch family encode large single-spanning transmembrane receptors that interact with membrane-bound ligands of the *Delta* and *Serrate*/*Jagged* family. After activation by a ligand, the Notch receptor is proteolytically cleaved, releasing the Notch intracellular domain (NICD) from the membrane. The NICD then translocates to the nucleus and interacts with the CSL DNA-binding protein (CBF1 or RBP-Jκ in vertebrates, Suppressor of hairless in *Drosophila melanogaster*, and Lag-1 in *Caenorhabditis elegans*) and the Mastermind/Lag-3 coactivator to activate target gene expression (27, 37). Spatiotemporal control of Notch signaling activity is achieved by numerous accessory proteins first identified in *Drosophila* and *C. elegans* (1, 37). Among them, a novel direct regulator of the Notch signaling pathway, called Notchless (Nle), has been identified in *Drosophila* during a genetic screen for suppressors of the *notchoid* mutant (36). Nle is composed of a well-conserved amino-terminal region, named Nle, and belongs to the WD40 repeat family of proteins. Members of this family interact with several protein partners and are involved in many cellular functions (40). An Nle-like amino-terminal domain was also found in another protein, named Wdr12, recently identified during a genetic screen for modulators of T-lymphocyte differentiation (29). The nuclear Wdr12 protein is composed of seven WD40 repeat domains, which, however, are not related to the WD40 domains of mouse Nle (mNle).

In *Drosophila*, a decrease of Nle expression suppresses the phenotype observed in the wings of the *notchoid* mutants, indicating that Nle reduces Notch activity (36). Furthermore, overexpression of Nle enhances the phenotype observed in *Drosophila* carrying Notch gain-of-function mutations and inhibits neuronal differentiation in *Xenopus laevis*. Hence, depending on the context, Nle either negatively or positively regulates the Notch pathway. Biochemical experiments showed that Nle binds to the NICD, but the molecular mechanism of action of Nle has yet to be clarified. Previously, Royet et al. also showed that Nle genetically interacts with other genes of the Notch pathway such as *Deltex*, *suppressor of hairless*, and *groucho* but not with *Serrate*, *Delta*, *Hairless*, or *strawberry notch* (36).

To obtain insights into the in vivo function of *Nle* in mammals, we genetically disrupted the *mNle* gene. Interestingly, we find that the absence of mNle results in peri-implantation lethality and demonstrate that *mNle* is a novel gene essential for the survival of inner cell mass (ICM) cells in mammals.

* Corresponding author. Mailing address: Unité Biologie du Développement, CNRS URA 2578, Institut Pasteur, Paris, France. Phone: 33 1 45 68 85 54. Fax: 33 1 45 68 86 34. E-mail: chbabi@pasteur.fr.

† Present address: Department of Biology, Johns Hopkins University, Baltimore, Md.

‡ Present address: Unité Biologie et Génétique du Paludisme, Institut Pasteur, Paris, France.

§ S.C. and S.L.B. contributed equally to this work.

MATERIALS AND METHODS

Northern blot. A specific probe corresponding to the open reading frame (ORF) of *mNle* was labeled with ^{32}P and used for hybridization in ExpressHyb buffer (Clontech) on adult and embryonic mouse multiple tissue Northern blots

(Clontech) using standard procedures. After stripping, membranes were rehybridized with a ^{32}P-labeled full-length murine *actine* cDNA probe.

***Xenopus laevis* embryo injections.** Synthetic capped RNAs for microinjection were synthesized by in vitro transcription using mMessage mMachine kit (Ambion) and purified according to the manufacturer's instructions. *mNle* and green fluorescent protein (*GFP*) RNAs were prepared from pRN3 derivatives, and *NICD* RNAs were prepared from pCS2 (kindly provided by A. Israël). *X. laevis* embryos were obtained by in vitro fertilization. Dorsal blastomeres of four-cell-stage embryos were injected with 100 pg of *GFP* capped RNAs alone or in combination with 100 pg of *mNle* or *NICD* RNAs. Expression of N-tubulin at the neural plate stage was analyzed by whole-mount in situ hybridization using digoxigenin-labeled probes, as described previously (6). Images were acquired using an SMZ1500 stereomicroscope (Nikon) equipped with an axioCam color camera (Zeiss).

Targeted disruption of the *mNle* gene. A 10.5-kb NdeI-HincII 129/Sv genomic DNA fragment, containing exons 1 to 13, was subcloned from clone 4B7 of the Caltech CITB-BAC library (GenBank accession no. AL713882) in pBKS(+). The BglI-BsrGI fragment was subcloned, and the PstI-EcoRV fragment was replaced by nlsLacZ (isolated from the plasmid pSKTNLSLACZ, a gift from S. Tajbakhsh) and floxed pgk-Neo cassettes (provided by P. Soriano). The targeted allele, *mNle*, and the pgk-Neo cassette are transcribed in the opposite orientation. The BsrGI-HincII fragment was then subcloned 3′ to the pgk-Neo cassette. A pgk-DTA cassette encoding the A subunit of the diphtheria toxin gene (provided by P. Soriano) was inserted at the 5′ end of the construct to allow for negative selection in embryonic stem (ES) cells (50). The resulting targeting vector was linearized at a unique XhoI site, gel purified, and electroporated (20 μg) (1 pulse of 0.23 kV and 950 μF, Gene PulserII; Bio-Rad) into 1.6×10^6 exponentially growing 129/Sv CK35 ES cells (22). ES cells were maintained, as described previously (34), in high-glucose Dulbecco's modified Eagle's medium supplemented with a solution containing 15% fetal calf serum, 0.1 mM β-mercaptoethanol, and 1 mM sodium pyruvate in the presence of 10^3 U/ml murine leukemia inhibitory factor (LIF). The cells were cultured on mitomycin C-treated Neo^r primary fibroblasts. Twenty hours after electroporation, ES cells were selected for G418 resistance (300 μg/ml; Invitrogen) for 10 days and genotyped. Genomic DNA was purified from G418-resistant ES cell clones, digested with BsrGI or EcoRV, transferred onto nitrocellulose membranes (Hybond N$^+$; Amersham), and hybridized with the 5′ and 3′ probes according to standard procedures. Southern blot analysis detected products of 12 kb and 7 kb using a 5′ probe and 16 kb and 12 kb using a 3′ probe for the targeted and wild-type (WT) alleles, respectively. ES cells exhibiting the correct targeting event were injected into C57BL/6N blastocysts which were transferred into (C57BL/6N × CBA)F1 pseudopregnant females. Resulting chimeric males were mated with C57BL/6N or 129/Sv females. Germ line transmission of the targeted *mNle* locus was confirmed by PCR that amplified a 269-bp fragment for the WT allele with primers a (5′-CTG GCG TTC TAT GTC CAC GAT G-3′) and b (5′-GGA TGG TCC TCT CCA CCT GTC-3′) and a 460-bp fragment for the mutant *mNle* allele with primers c (5′-GAC TAG GGG AGG AGT AGA AGG T-3′) and b. The PCR amplification protocol was as follows: 94°C for 5 min followed by 33 cycles at 94°C for 30 s, 60°C for 30 s, and 72°C for 30 s.

Early embryo isolation and in vitro cultures. Heterozygous *mNle*$^{+/-}$ females, obtained from crosses between WT (C57BL/6 × SJL/J) females and *mNle*$^{+/-}$ 129/Sv males, were superovulated by injection of 5 units of pregnant mare serum gonadotrophin (Calbiochem) followed by injection of 5 units of human chorionic gonadotrophin (Intervet) 48 h later and were then mated with heterozygous *mNle*$^{+/-}$ 129/Sv males. The next day, successful matings were detected by the presence of a vaginal plug. Embryos were collected from different stages of development (embryonic day 1.5 [E1.5] through E2.5) by either dissecting ampullae or flushing oviducts with PB1 medium (48). E3.5 blastocysts were collected by flushing uteri with ES cell medium without LIF and supplemented with 20 mM HEPES. When mentioned, zona pellucida was removed from E3.5 blastocysts with acid Tyrode's solution. E3.5 blastocysts from *mNle*$^{+/-}$ intercrosses were transferred in ES cell medium without LIF onto 0.1% gelatin-coated chambered slides (Lab-Tek) at 37°C with 8% CO_2 during 24 h and for up to 7 days and photographed every 24 h (DMIL; Leica) (Coolpix990; Nikon). Immunosurgical isolation of inner cell populations was carried out, as previously described (41), on E3.5 blastocysts cultured in vitro during 24 h. Inner cell clumps were cultured in ES cell medium without LIF for 7 days. Preimplantation embryos or TE lysates were incubated in lysis buffer (10 mM Tris, pH 8.5, 50 mM KCl, 0.01% gelatin, 300 μg/ml proteinase K) at 55°C for 60 min and 95°C for 15 min, and the genotype was assessed by nested PCR. The first round of PCR amplification used primers b, c, and d (5′-GAC GTG CAG CGG CTG CTC GTA-3′) for 25 cycles at 94°C for 30 s, 60°C for 30 s, and 72°C for 40 s. The second round of PCR amplification for 25 cycles used primers a, e (5′-GGG CTG CTA AAG CGC ATG CT), and f (5′-CTT CGC TGT GAC CCT CCA ATG-3′).

Immunofluorescence and TUNEL assay. Immunofluorescence and terminal deoxynucleotidyltransferase-mediated dUTP-biotin nick end labeling (TUNEL) assay were performed as described previously (3) on fully expanded E3.5 blastocysts cultured in vitro during 24 h. The antibodies used were as follows: anti-cytokeratin-Endo-A (TROMA-1; 1:100; DSHB clone SP2/0), anti-CDX2 (1/50; BioGenex), anti-Oct-3/4 (1:300; BD Biosciences), anti-phospho-histone H3 (1:100; Upstate), anti-active human caspase 3 (1:200; Pharmingen), Alexa 488-nm–anti-rabbit antibody (1:100; Molecular Probes), and Alexa 594-nm–anti-mouse antibody (1:200; Molecular Probes).

X-Gal staining. After fixation of embryos, β-galactosidase expression was visualized by staining with 5-bromo-4-chloro-3-indolyl-β-D-galactopyranoside (X-Gal for embryos; Life Technologies).

Histological analysis. Uteri containing E5.5 and E6.5 decidual swellings were fixed for 24 h in Bouin's solution (Sigma) and then dehydrated and embedded in paraffin. Next, 5-μm sections were stained with hematoxylin and eosin.

RESULTS

Characterization of the *mNle* gene. We isolated the *mNle* gene (GenBank accession no. NM_145431) during the positional cloning of the *Ovum mutant* locus responsible for a conditional preimplantation lethal syndrome, called DDK syndrome (4, 7, 25). The *mNle* gene contains 13 exons and encodes a protein of 485 amino acids. mNle consists of the Nle amino-terminal domain followed by WD40 repeat domains (Fig. 1A and B) and presents 51% and 96% identity with yeast and human Nle proteins, respectively. In *Drosophila*, Royet et al. proposed previously that Nle contains nine WD40 repeat domains (36). However, our analysis suggests that all Nle orthologous proteins actually contain eight WD40 domains (Fig. 1B). Northern blot experiments revealed that a single *mNle*-specific transcript of approximately 2 kb was present in embryos and in all adult tissues tested (Fig. 1C).

mNle has conserved its ability to modulate Notch activity. The *Xenopus* neuronal specification assay (6) was used to test whether the described activity of *Xenopus* and *Drosophila* Nle proteins as modulators of the Notch signaling pathway (36) was conserved in mouse. Indeed, the formation of primary neurons can be used as a readout of Notch signaling in *Xenopus*: inhibition of Notch signaling results in an overproduction of primary neurons, while an increase in Notch signaling leads to a marked reduction in the differentiation of primary neurons (6). Thus, we injected a single dorsal blastomere of four-cell-stage embryos with *GFP* RNAs alone or in combination with *mNle* or *NICD* RNAs. Correctly injected embryos were identified based on GFP expression at the neurula stage (stage 16) and processed for N-tubulin, which marks primary neurons in medial, intermediate, and lateral stripes (Fig. 2B). When embryos were injected with *mNle* mRNAs, a significantly higher proportion of embryos showed a reduced or complete loss of primary neurons in the three neural stripes compared to *GFP*-injected embryos (Fig. 2A). This reduction is indicative of activated Notch signaling (6) and is similar to that observed when embryos were injected with NICD (Fig. 2). This result strongly suggests that the murine Nle protein has the capacity to modulate the Notch signaling activity, as it is the case for its fly and frog orthologs (36).

Targeted disruption of the *mNle* gene. To elucidate the in vivo function of *mNle*, we disrupted it via homologous recombination in 129/Sv ES cells by an in-frame insertion of the *nlsLacZ* ORF (Fig. 3A). This insertion was expected to result

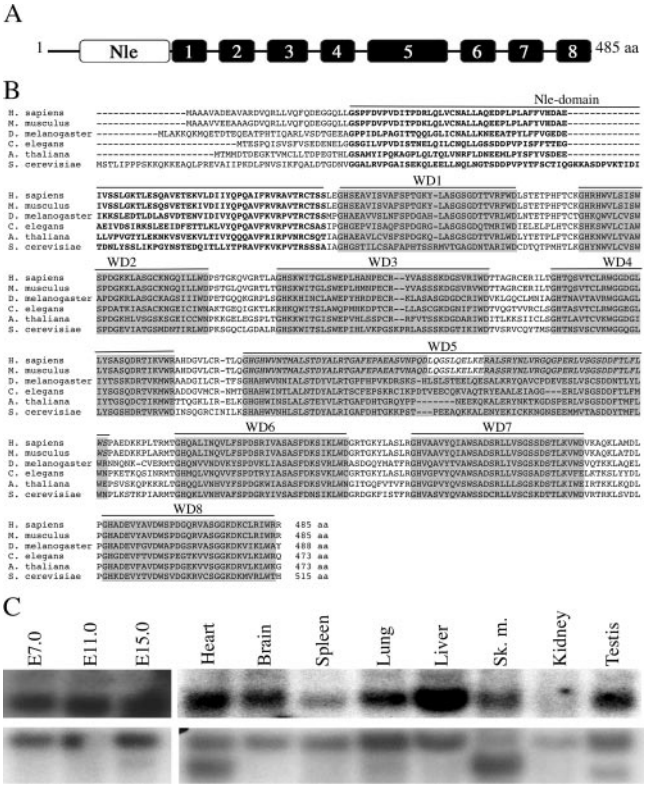

FIG. 1. Structure and amino acid alignments of mNle protein and expression pattern of *mNle* transcripts. (A) Schematic representation of the mNle protein containing a single Nle domain (white box) at its amino-terminal region and eight WD40 domains (gray boxes). (B) Alignments of sequences of Nle orthologs by clustalW. Using the website at http://bmerc-www.bu.edu/wdrepeat to search for WD40 domains, eight domains were predicted for Nle in *Saccharomyces*, *Xenopus*, and *Drosophila*, whereas nine domains were predicted for mouse and human Nle proteins. Based on amino acid sequence comparisons and on the fact that, in mouse and human, the fifth domain does not end by a consensus WD motif and that the sixth domain does not begin by a consensus GH sequence, we propose that the fifth and sixth predicted WD40 domains of the human and mouse Nle proteins correspond to a single WD40 domain (in italics), as predicted for other species. GenBank/EMBL accession numbers for the Nle orthologous sequences are as follows: *Homo sapiens*, NP_060566; *Mus musculus*, NP_663406; *D. melanogaster*, NP_477294.1; *C. elegans*, NP_493745; *Arabidopsis thaliana*, NP_200094.1; and *S. cerevisiae*, NP_009997. Amino acids corresponding to the Nle domain are in boldface type. WD40 repeat domains are highlighted in gray boxes. The numbers of amino acids (aa) are indicated at the end of the sequences. (C) Northern blot analysis of poly(A)$^+$ mRNAs of embryos at E7.0 to E15.0 and various adult tissues hybridized with an *mNle*-specific probe (upper panel) or a β-*actin* probe (lower panel).

in a null allele, since it deletes exons 2 and 3 and results in the fusion of the first six amino acids of the Nle protein to the ORF of *nlsLacZ*. Correctly targeted clones were identified by Southern blot analysis (Fig. 3B). Modified cells were injected into C57BL/6 blastocysts, and germ line transmission of the *mNle*-targeted allele was obtained. The phenotype described below was fully penetrant on a mixed 129/Sv × (C57BL/6 × SJL/J) genetic background.

***mNle* gene disruption results in peri-implantation lethality and ICM cell failure.** Males and females heterozygous for the *mNle*-null allele were not phenotypically different from the

A

Injected RNAs	No change	Reduction	Complete loss	Total of scored embryos
GFP (100 pg)	21	6	0	27
NICD (100 pg)*	2	3	5	10
mNle (100 pg)*	0	8	3	11

B

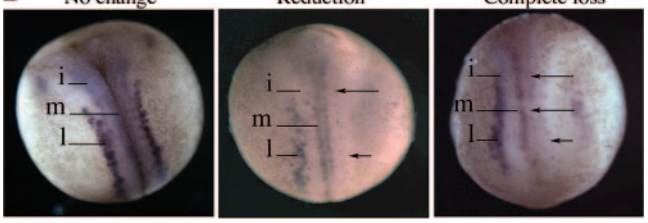

FIG. 2. Effect of *GFP*, *NICD*, and *mNle* RNA injections on the production of primary neurons in *Xenopus* embryos. Injected embryos (stage 16) were monitored for the N-tubulin expression pattern. (A) Number of embryos that present, in the injected side compared to the noninjected side, no change, reduction, or complete loss of N-tubulin-positive neurons. ∗, analysis of distribution of the three N-tubulin expression profiles between *NICD* and *GFP* (χ^2, $0.001 < P < 0.01$) and between *mNle* and *GFP* (χ^2, $P < 0.001$). (B) Examples of the three types of N-tubulin expression patterns obtained after RNA injections. Dorsal views are shown with the anterior end up. The injected side is shown on the right side of the images. N-tubulin expression was detected in primary neurons of medial (m), intermediate (i), and lateral (l) stripes in the noninjected side. Arrows indicate the reduction or complete loss of N-tubulin expression.

wild-type mice. When *mNle*$^{+/-}$ mice were intercrossed, no homozygous progeny were found among 68 newborns (Table 1), indicating that homozygosity for the *mNle*-null allele is lethal during embryonic development. Similarly, no homozygous embryos could be found from E12.5 to as early as E6.5. By contrast, a Mendelian distribution was observed at E3.5 for *mNle*$^{+/+}$, *mNle*$^{+/-}$, and *mNle*$^{-/-}$ embryos (Table 1 and Fig. 3C). To further precise the time of embryonic death, we performed a histological analysis of serial sections of E5.5 and E6.5 decidual swellings from *mNle*$^{+/-}$ intercrosses. For both gestation times, abnormal implants that contained very few cells and no discernible embryonic tissue were observed (Table 2 and data not shown). As the frequency of such abnormal deciduae was much lower in control crosses, they were considered to be elicited from *mNle*$^{-/-}$ embryos. We conclude from these results that *mNle*$^{-/-}$ embryos do implant but rapidly degenerate thereafter.

The developmental status of mutant blastocysts was then examined by in vitro culture experiments. At the time of harvest, homozygous E3.5 blastocysts were indistinguishable from their heterozygous and wild-type counterparts (Fig. 4). After 3 days in culture, *mNle*$^{+/+}$ and *mNle*$^{+/-}$ blastocysts had hatched from the zona, ICMs had increased in size, and TE had proliferated and differentiated into giant cells (Fig. 4A). In contrast, the null blastocysts behaved differently in this assay. The majority of null blastocysts (17 out of 21) failed to hatch and degenerated rapidly inside the zona pellucida (Fig. 4C). The remaining null embryos hatched, adhered to the culture dish, and yielded apparently normal giant trophoblast cells but did not contain any recognizable ICM-derived structure after 2 days (Fig. 4B). This latter phenotype was observed for all

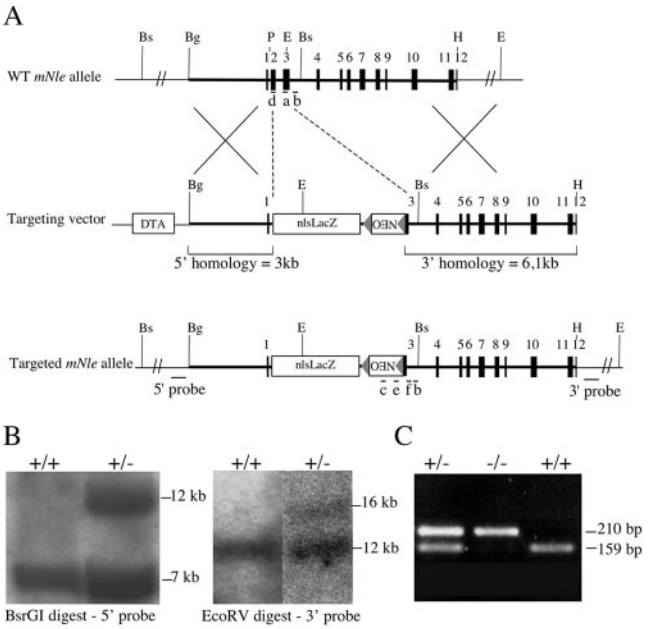

FIG. 3. Targeted disruption of the *mNle* gene. (A) Structure of the WT *mNle* allele, the targeting vector, and the targeted allele. Exons (solid boxes), LoxP sequences (triangles), and positions of primers used for genotype analysis (a to f, bars), probes used for Southern blot analysis (bars), and pgk-DTA and pgk-Neo cassettes used for negative and positive selection are indicated. Restriction sites relevant to the targeting construct and to the screening strategies are as follows: BglI (Bg), BsrGI (Bs), EcoRV (E), HincII (H), and PstI (P). (B) Southern blot analysis of genomic DNA obtained from wild-type and heterozygous ES cells. (C) Genotype analysis of early embryos from $mNle^{+/-}$ intercrosses. The first round of PCR used primers b, c, and d. The second round of PCR used primers a, e, and f, yielding amplification products of 159 bp and 210 bp for the wild-type and mutant alleles, respectively.

mNle-deficient blastocysts when the zona pellucida was chemically removed at E3.5 ($n = 21$). After 7 days of culture, the giant trophoblast cells were still present in null outgrowths, but they occupied a threefold smaller area than in controls (data not shown). This is likely to be due to the absence of ICM, as interactions between ICM and TE are known to be essential for a harmonious development of the two lineages (35). We also tested whether degenerescence of ICM cells could be due to defective interactions with TE in *mNle*-deficient embryos. To do this, ICMs of E3.5 blastocysts harvested from $mNle^{+/-}$ intercrosses and cultured for 24 h (called E4.5 blastocysts hereafter) were isolated by immunosurgery and cultured for 7 days.

TABLE 1. Viability analysis of $mNle^{-/-}$ mouse and embryos[a]

Time of analysis	No. (%) of live births and dissected embryos from $mNle^{+/-}$ intercrosses from genotype:		
	+/+	+/−	−/−
Postnatal	22 (32)	46 (68)	0
E10.5–E12.5	14 (29)	34 (71)	0
E6.5	9 (29)	22 (71)	0
E3.5	13 (20)	39 (59)	14 (21)

[a] Mice and E6.5 to E12.5 embryos were genotyped by PCR, and E3.5 embryos were genotyped by nested PCR (see Fig. 3C).

TABLE 2. Histological analysis of embryos in utero[a]

Cross	Stage	No. of embryos		
		Total	Normal	Resorbed
$mNle^{+/-} \times mNle^{+/-}$	E5.5	9	6	3
$mNle^{+/-} \times mNle^{+/-}$	E6.5	18	11	7
$mNle^{+/+} \times mNle^{+/-}$	E5.5	6	6	0
$mNle^{+/+} \times mNle^{+/-}$	E6.5	16	15	1

[a] For histological analysis, uteri were fixed, sectioned and stained with hematoxylin and eosin, and scored as normal or resorbed based on presence or absence of embryos and general morphology.

Most of $mNle^{+/+}$ and $mNle^{+/-}$ ICMs proliferated and gave rise to endodermal cells (Table 3). In contrast, inner cells from $mNle^{-/-}$ embryos did not survive after 24 h of culture. This result suggested that the absence of mNle causes ICM cell death in a cell-autonomous manner. Altogether, these results indicate that *mNle* disruption results in the absence of ICM derivatives and embryonic death shortly after implantation.

Specification of early embryonic lineages in the absence of mNle. The observation that ICM development is compromised in $mNle^{-/-}$ embryos to a greater extent than TE led us to assess *mNle* gene expression in early embryos. To do this, we took advantage of the *nlsLacZ* insertion and stained heterozygous embryos with X-Gal at various stages. We observed that zygotic transcription of *mNle* occurred at the two-cell stage, at the time of major zygotic gene activation (Fig. 5A). In blastocysts, X-Gal staining was found to be more intense in the ICM than in the TE (Fig. 5B). After implantation, β-galactosidase-expressing cells were observed mainly in the embryonic tissue derived from the ICM (Fig. 5C). Thus, the expression pattern of the *mNle*-targeted allele is consistent with mNle being preferentially required for the formation of ICM derivatives.

We then examined TE and ICM specification in *mNle*-deficient embryos using specific markers. Analysis was performed on E4.5 blastocysts, i.e., 1 day before degenerescence of *mNle*-deficient ICMs (Fig. 4). To examine TE specification, we analyzed the expression pattern of Endo-A cytokeratin, an intermediate filament of the type II cytokeratin class, and Cdx2, a transcription factor required for establishment and function of the TE (42). Both Endo-A and Cdx2 can be detected in the eight-cell morulae, and their expression became tightly restricted to the TE at the blastocyst stage (5, 42). We observed that Endo-A and Cdx2 expression was restricted to the TE of $mNle^{+/+}$, $mNle^{+/-}$, and $mNle^{-/-}$ E4.5 embryos (Fig. 6A), suggesting that correct specification of TE occurred in mNle-deficient embryos. To monitor ICM specification, we looked at the expression pattern of Oct4, a transcription factor essential for the maintenance of pluripotency in ICM (30). Initially present in the nuclei of all cells, Oct4 protein becomes progressively restricted to the ICM during blastocyst differentiation (26, 32). When $mNle^{+/-}$-intercrossed embryos were immunostained with a specific anti-Oct4 antibody, we observed that the majority of control embryos (72%; $n = 53$) exhibited ICM-restricted expression (Fig. 6C, upper panel). In the remaining $mNle^{+/+}$ and $mNle^{+/-}$ embryos, staining in all the cells (ICM and TE) was observed; nevertheless, staining in TE cells was less intense than that in ICM cells (data not shown). This is likely to reflect a developmental asynchrony between

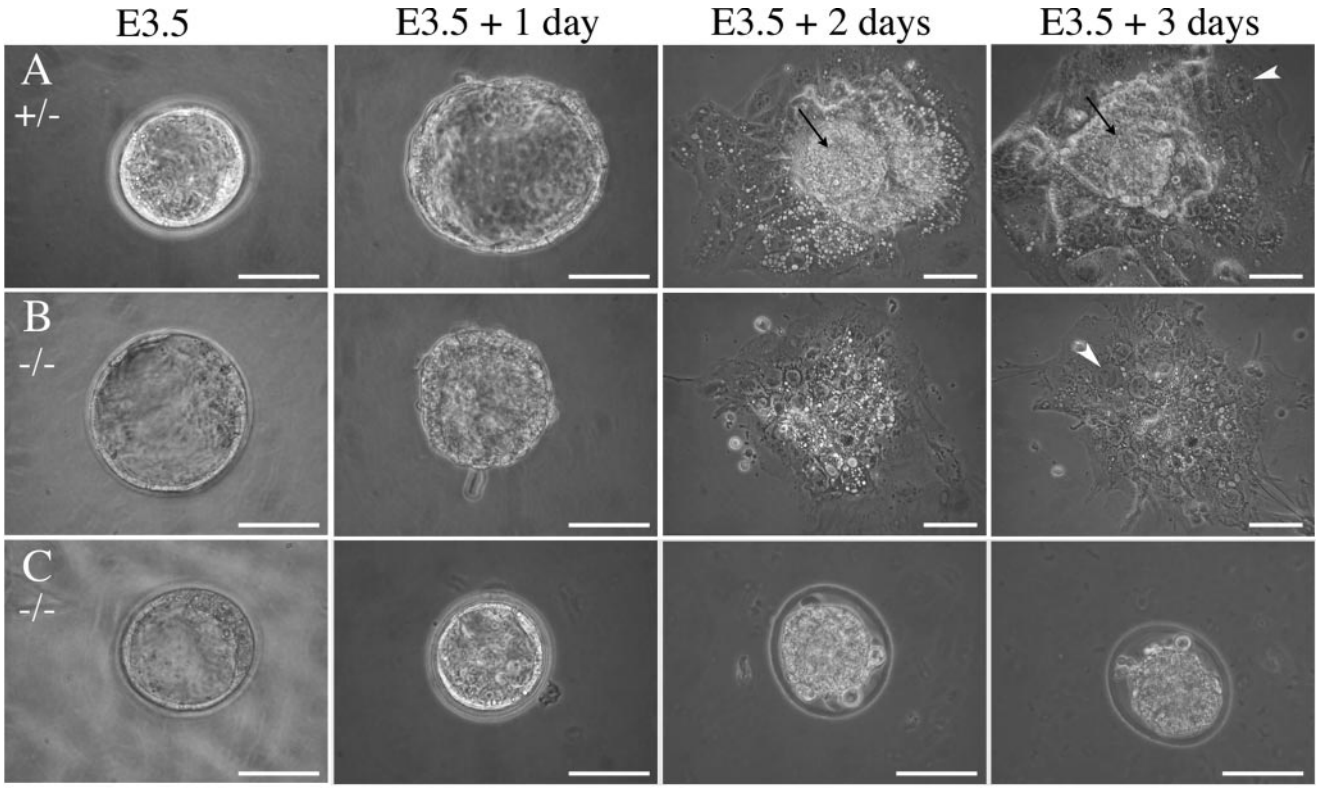

FIG. 4. Cultures of embryos derived from *mNle*$^{+/-}$ intercrosses. E3.5 blastocysts were harvested and cultured for 3 days. *mNle*$^{+/+}$ and *mNle*$^{+/-}$ blastocysts (A) hatched from the zona pellucida after 1 day and attached to the culture dish. During the following days, the ICM proliferated (arrows) and the trophectoderm differentiated (arrowheads). *mNle*$^{-/-}$ blastocysts were indistinguishable from controls at E3.5 (B and C). After 24 h in vitro, most of them were unable to hatch from the zona (C) and degenerated rapidly. The remaining *mNle*$^{-/-}$ embryos hatched (B) and attached to the dish, and the trophectoderm expanded and differentiated (arrowhead). However, after 2 days in culture, the ICM degenerated and was no longer discernible. Bars, 50 μm.

embryos. Interestingly, the reverse situation was observed for *mNle*-null embryos. Indeed, 35% of *mNle*$^{-/-}$ embryos exhibited ICM-restricted expression of Oct4, while 65% exhibited expression in all the cells ($n = 26$; $P < 0.01$, χ^2 test) (Fig. 6C, lower panel). After 3 days in culture, only the few remaining ICM cells of *mNle*$^{-/-}$ blastocyst outgrowths stained positively for Oct4, indicating that *Oct4* gene expression has been turned off in trophoblastic cells (Fig. 6D). These data suggest that *mNle* deficiency does not impair ICM specification but results in a delay of down-regulation of Oct4 in the TE.

The absence of mNle results in ICM cell apoptosis. The observation that *mNle*$^{-/-}$ ICMs degenerate in culture led us to analyze cell proliferation and death in E4.5 blastocysts in more detail. First, the number of TE cells (external layer of cells) and ICM cells (internal cells with strong Oct4-positive signal) was determined by counting the number of nuclei stained with Hoechst stain in serial optical sections. No difference in the number of TE cells between the three genotypes was observed (Table 4). In contrast, the number of ICM cells in *mNle*-deficient embryos was significantly lower than that in control embryos (Table 4) ($P < 0.0001$, analysis of variance [ANOVA] test) (this reduction can also be visualized in Fig. 6). We next

TABLE 3. Culture of ICMs from *mNle*$^{+/-}$ intercrosses

Phenotype	No. (%) with genotype:		
	+/+	+/−	−/−[a]
Outgrowth	16 (84)	31 (89)	0
No survival	3 (16)	4 (11)	20 (100)[b]

[a] χ^2, $P < 0.001$.
[b] One *mNle*$^{-/-}$ ICM gave rise to few endoderm-like cells.

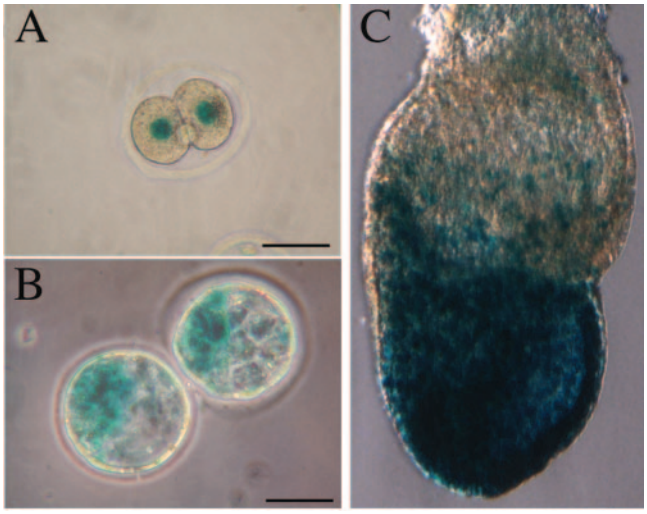

FIG. 5. *nlsLacZ* expression pattern in *mNle*$^{+/-}$ heterozygous early embryos. X-Gal staining was performed on embryos harvested from crosses of wild-type females and heterozygous males at E1.5 (A), E3.5 (B), and at late bud stage (C). Scale bars, 50 μm.

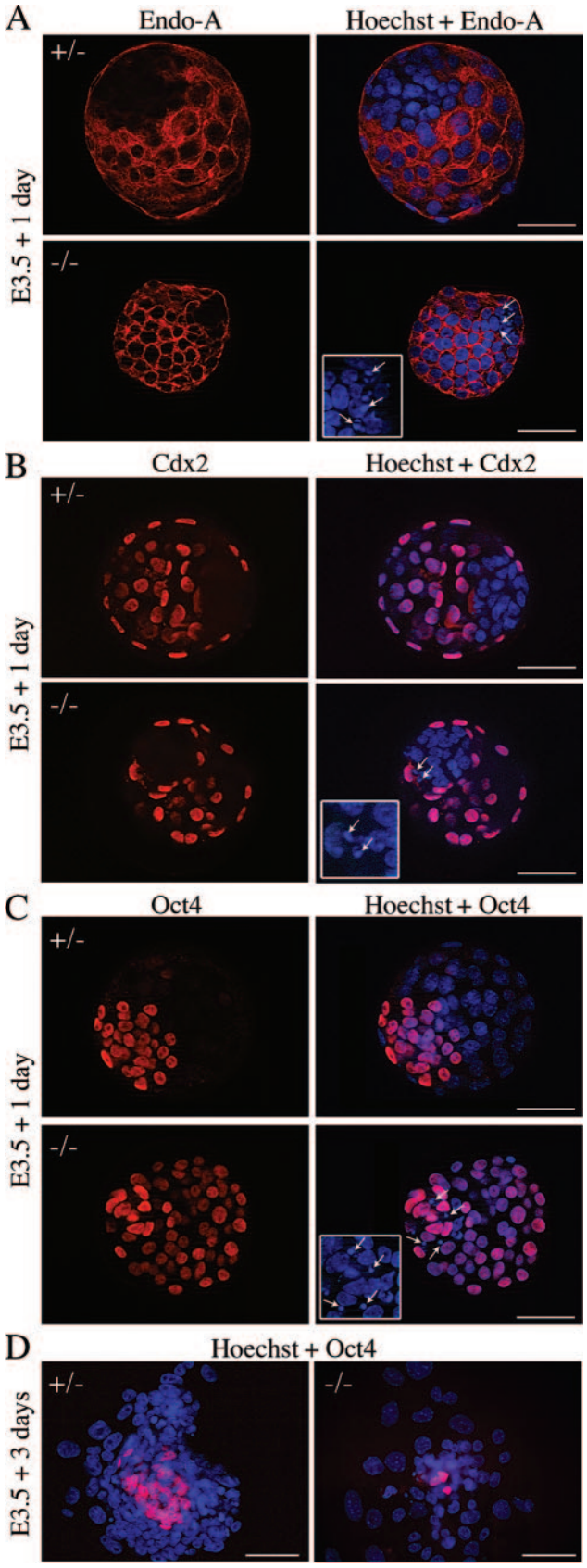

FIG. 6. TE and ICM specification in E4.5 blastocysts and outgrowths from *mNle*$^{+/-}$ intercrosses. Immunohistochemical detection of cytoplasmic Endo-A cytokeratin (red) (A) and nuclear Cdx2 (red) (B), specific for TE, and nuclear Oct4 (red) (C), specific for ICM, in *mNle*$^{+/-}$ and *mNle*$^{-/-}$ embryos is shown. Representative control embryos (upper panel) and *mNle*$^{-/-}$ embryos (lower panel) are shown. (D) Oct4 expression in *mNle*$^{+/-}$ and *mNle*$^{-/-}$ outgrowths from blastocysts cultured for 3 days. In *mNle*$^{+/-}$ outgrowths, Oct4-positive immunostaining was detected in the ICM. In contrast, very few Oct4-positive cells were observed in *mNle*$^{-/-}$ outgrowths. Nuclei were counterstained with Hoechst stain (blue). One optical section is shown for panels A to C (flattened blastocyst morphology was due to mounting on one slide with a glass coverslip placed over it). Micronuclei were detected in the ICM of the *mNle*$^{-/-}$ blastocysts (white arrows and insets, panels A to C). Bars, 50 μm (panels A to C) and 200 μm (panel D).

TABLE 4. Differential count of ICM and TE nuclei in E3.5 blastocysts from *mNle*$^{+/-}$ intercrosses cultured for 24 h

Type	No. ± SEM of nuclei (no. of embryos) with genotype:		
	+/+	+/−	−/−
ICM	29.5 ± 3.0 (8)	27.7 ± 1.5 (20)	14.4 ± 1.2[a] (11)
TE	58.9 ± 2.2 (8)	60.6 ± 2.0 (17)	56.1 ± 5.2 (9)

[a] $n = 39$; $P < 0.0001$, ANOVA test.

examined cell proliferation and cell death status. The histone H3 phosphorylation on serine residue 10 was examined to determine the number of cells in M phase (16). No difference was observed in E4.5 *mNle*$^{-/-}$ embryos compared with controls, indicating that the absence of mNle does not impair proliferation. To address a possible effect of the absence of mNle on apoptosis, we then performed microscopic examination of nuclear staining with Hoechst stain as well as TUNEL analysis. As shown in Fig. 6 (insets), *mNle*$^{-/-}$ E4.5 blastocysts exhibited an abnormally high number of condensed micronuclei. Fragmented DNA was observed essentially in the ICM and more rarely in the TE. The percentage of *mNle*$^{-/-}$ blastocysts yielding micronuclei was significantly higher than that observed for *mNle*$^{+/-}$ and *mNle*$^{+/+}$ blastocysts (83% for *mNle*$^{-/-}$ blastocysts compared to 39% and 33% for *mNle*$^{+/-}$ and *mNle*$^{+/+}$ blastocysts, respectively) (Fig. 7A). Next, a TUNEL assay was performed, which showed a twofold increase of TUNEL-positive cells in *mNle*$^{-/-}$ embryos compared to *mNle*$^{+/-}$ and *mNle*$^{+/+}$ embryos (5.3 ± 0.6 compared to 2.2 ± 0.4 and 2.4 ± 0.4, respectively) (Fig. 7B). Apoptosis was further analyzed by evaluating the caspase 3-dependent apoptotic process. To do this, we performed immunostaining of E4.5 *mNle*$^{+/-}$-intercrossed embryos using a specific antibody recognizing the active form of caspase 3. The percentage of caspase 3-positive *mNle*$^{-/-}$ embryos was significantly greater than those of the *mNle*$^{+/-}$ and *mNle*$^{+/+}$ embryos (73% compared with 24% and 13%, respectively) (Fig. 7C). It is noteworthy that no significant difference could be found between the three genotypes regarding the percentage of micronucleus-containing and caspase 3-positive embryos a day earlier (E3.5 blastocysts) (not shown). Altogether, these data indicate that caspase 3-dependent apoptotic cell death largely contributes to embryonic lethality in *mNle*$^{-/-}$ embryos.

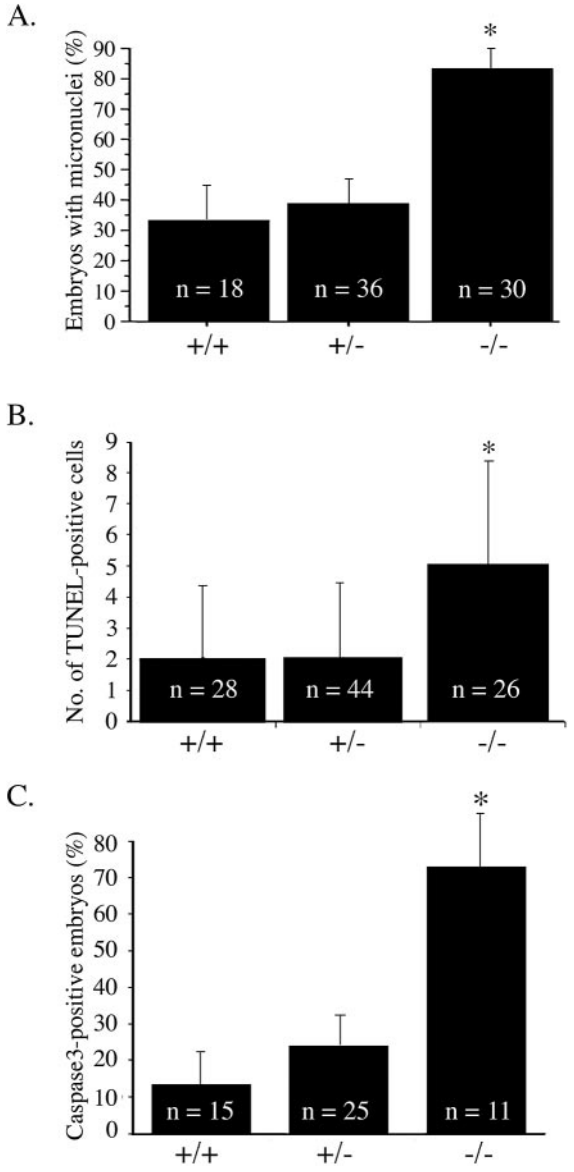

FIG. 7. Apoptosis in E3.5 blastocysts from $mNle^{+/-}$ intercrosses cultured for 24 h. (A) Percentage of $mNle^{+/+}$, $mNle^{+/-}$, and $mNle^{-/-}$ embryos yielding micronuclei detected by Hoechst reagent staining ($n = 84$; $P < 0.001$, χ^2 test). Data ± standard errors of the means (bars) are shown. (B) A twofold increase of TUNEL-positive cells was observed in $mNle^{-/-}$ blastocysts compared with control counterparts ($n = 90$; $P < 0.0001$, ANOVA test). Data ± standard deviations (bars) are shown. (C) Percentage of $mNle^{+/+}$, $mNle^{+/-}$, and $mNle^{-/-}$ embryos positive for the active form of caspase 3 protein ($n = 51$; $P < 0.01$, χ^2 test). Data ± standard errors of the means (bars) are shown. Asterisks indicate statistical difference.

DISCUSSION

Nle is a well-conserved protein found from yeast to humans. In *Drosophila*, Nle binds to the intracellular domain of the Notch receptor and has been demonstrated to be either a positive or a negative regulator of the Notch signaling pathway (36). There are very few reports concerning the role of Nle in species other than *Drosophila* and *Xenopus*. In *Saccharomyces cerevisiae*, large-scale deletion studies suggest that the loss of Nle, referred to as YCR072C, is lethal (11). Because genes encoding the Notch receptors and their ligands are absent in yeast, this phenotype might account for an ancestral function of Nle. In *C. elegans*, large-scale RNA interference experiments indicate that the absence of Nle does not alter embryonic development but leads to slow growth and patchy coloration, larval arrest, or egg-laying defects (20, 39). However, it is not known whether these phenotypes are due to a dysregulation of the Notch pathway. Importantly, our study is the first to define the role of Nle in mammals.

Disruption of the *mNle* gene leads to embryonic lethality shortly after implantation. *mNle*-null blastocysts implant into the uterine wall but do not progress much further. In particular, no epiblast or extraembryonic ectoderm could be recognized in E5.5 implantation sites elicited by $mNle^{-/-}$ embryos, suggesting early failure of ICM derivatives. Consistent with this, ICM cells did not survive in $mNle^{-/-}$ blastocyst outgrowths. Thus, the absence of mNle prevents the ICM cells from thriving both in vivo and in vitro, indicating that mNle is instrumental for their survival. In mutant embryos, ICM cells degenerate, while TE is able to induce a decidual reaction and to differentiate normally during the initial steps of blastocyst outgrowth, suggesting that *mNle* function is required mainly in ICM cells. Supporting this idea is the observation that zygotic *mNle* expression, monitored via the *nlslacZ* knock-in allele, is stronger in the ICM than in the TE. However, we cannot formally exclude that *mNle*-null ICM failure is a consequence of abnormal interactions between inner and outer cells earlier in development. It should nevertheless be noted that E3.5 *mNle*-deficient blastocysts cannot be distinguished from their wild-type or heterozygous counterparts either by gross morphological examination or through counting inner and outer cell numbers. It should also be noted that *mNle* is expressed in oocytes (25), and therefore, maternally supplied *mNle* products might have obscured an eventual requirement for *mNle* function before the blastocyst stage.

mNle-deficient ICM failure does not seem to result from lineage specification defects. Indeed, we showed that these cells express, before they degenerate, high levels of Oct4 protein and are negative for Cdx2 and Endo-A immunoreactivity. Interestingly, the persistence of the Oct4 protein in the TE was observed in an abnormally high proportion of E4.5 *mNle*-deficient embryos, suggesting a delay in the temporal down-regulation of Oct4 in the trophectoderm lineage. As Oct4 and Cdx2 have recently been shown to form a repressor complex in ES cells (31), this observation raises the possibility that the TE would not be correctly specified in the absence of *mNle*. However, this is not supported by our observation that the *mNle*-deficient TE exhibited robust differentiation and functional capabilities. Altogether, these results indicate that mNle is dispensable for ICM and TE specification but is essential for the survival of ICM cells.

Apoptosis is an essential feature of many normal and pathological processes and takes place in normal mammalian preimplantation embryos. It has been proposed that apoptosis allows the elimination of ICM cells that retain trophectodermal potential and contributes to the threshold number of ICM cells compatible with a correct development of the embryo (15, 19, 33). In E4.5 $mNle^{-/-}$ blastocysts, ICM cells were shown to degenerate through a caspase 3-dependent apoptotic process.

Selective apoptosis of ICM at the peri-implantation period has been observed in mice disrupted for various genes, including genes involved in the control of the cell cycle (10, 43), the proteasome, and the ubiquitin-like conjugation pathway (28, 44, 45) or a novel gene of unknown function (47). Whether mNle is a direct regulator of apoptosis or *mNle*-deficient embryos died of apoptosis as a consequence of some severe defect directly caused by the absence of mNle remains to be clarified.

In the present study, we show that the murine Nle protein has the ability to modulate Notch signaling and that its deficiency results in lethality at the peri-implantation period. Together with the recent demonstration that various components of the Notch pathway are expressed in oocytes and preimplantation embryos (9), these data raise the possibility that the death of *mNle*-deficient embryos might result from abnormal Notch signaling during the first steps of development. Interestingly, disruption of the murine ortholog of *brainiac*, which interacts with the Notch pathway and plays a role in follicular epithelium morphogenesis in *Drosophila* (12, 13), results in embryonic lethality by the time of implantation (46), which also might signify an implication of Notch signaling in peri-implantation development. However, the phenotypes of *mNle*- and *brainiac*-null mice are very different from phenotypes of mice knocked out for core components of the Notch signaling cascade (for examples, see references 8, 14, 17, 18, 21, 23, 38, and 49). The absence of phenotypes during preimplantation development for some of the latter mutants could be due to maternally inherited products that might have overcome zygotic gene disruption (9). However, normal preimplantation development of embryos lacking both maternal and zygotic expression of either RBP-Jκ (C. Souilhol, S. Cormier, S. Vandormael-Pournin, C. Babinet, and M. Cohen-Tannoudji, unpublished data) or *O-fut* (37a), two essential components of the Notch pathway, strongly indicates that the canonical RBP-Jκ-dependent Notch pathway is dispensable for preimplantation development. Therefore, decreased Notch signaling activity cannot be the cause of *mNle*-deficient embryo lethality. Alternatively, a loss of mNle might result in an increased RBP-Jκ-dependent Notch signaling activity, as shown in *Drosophila* wing imaginal disks (36), which would in turn lead to compromised development. Another possibility would be that mNle is acting on an RBP-Jκ-independent Notch pathway during mouse preimplantation development. Future work will be necessary to determine whether either of these two possibilities might account for the death of *mNle*-null embryos at the time of implantation.

ACKNOWLEDGMENTS

We thank J. Artus, S. Tajbakhsh, J. Hadchouel, F. Relaix, and C. Brou for helpful discussions, C. Kress for her invaluable help and instruction with culture and manipulation of ES cells, and S. Lecorre for technical help. We acknowledge the dynamic imaging platform, Institut Pasteur, for helpful assistance.

This work was supported by the Centre National de la Recherche Scientifique (CNRS), the Association pour la Recherche contre le Cancer (ARC), the Institut Pasteur GPH07 on stem cells, and the Action concertée incitative Biologie du Développement et Physiologie Intégrative from the Ministère de l'Education Nationale, de la Recherche, et de la Technologie. S.C. received grants from the Pasteur-Negri-Weizmann Council and the ARC. S.L.B. received funding from the Ministere de l'Education Nationale and was a recipient of funding from the ARC. C.S. received grants from CNRS (Bourse de Doctorat pour les Ingénieurs).

REFERENCES

1. **Artavanis-Tsakonas, S., K. Matsuno, and M. E. Fortini.** 1995. Notch signaling. Science **268:**225–232.
2. **Artavanis-Tsakonas, S., M. D. Rand, and R. J. Lake.** 1999. Notch signaling: cell fate control and signal integration in development. Science **284:**770–776.
3. **Artus, J., S. Vandormael-Pournin, M. Frodin, K. Nacerddine, C. Babinet, and M. Cohen-Tannoudji.** 2005. Impaired mitotic progression and preimplantation lethality in mice lacking OMCG1, a new evolutionarily conserved nuclear protein. Mol. Cell. Biol. **25:**6289–6302.
4. **Babinet, C., V. Richoux, J. L. Guenet, and J. P. Renard.** 1990. The DDK inbred strain as a model for the study of interactions between parental genomes and egg cytoplasm in mouse preimplantation development. Dev. Suppl. **1990:**81–87.
5. **Chisholm, J. C., and E. Houliston.** 1987. Cytokeratin filament assembly in the preimplantation mouse embryo. Development **101:**565–582.
6. **Chitnis, A. B.** 1995. The role of Notch in lateral inhibition and cell fate specification. Mol. Cell. Neurosci. **6:**311–321.
7. **Cohen-Tannoudji, M., S. Vandormael-Pournin, S. Le Bras, F. Coumailleau, C. Babinet, and P. Baldacci.** 2000. A 2-Mb YAC/BAC-based physical map of the ovum mutant (Om) locus region on mouse chromosome 11. Genomics **68:**273–282.
8. **Conlon, R. A., A. G. Reaume, and J. Rossant.** 1995. Notch1 is required for the coordinate segmentation of somites. Development **121:**1533–1545.
9. **Cormier, S., S. Vandormael-Pournin, C. Babinet, and M. Cohen-Tannoudji.** 2004. Developmental expression of the Notch signaling pathway genes during mouse preimplantation development. Gene Expr. Patterns **4:**713–717.
10. **Dobles, M., V. Liberal, M. L. Scott, R. Benezra, and P. K. Sorger.** 2000. Chromosome missegregation and apoptosis in mice lacking the mitotic checkpoint protein Mad2. Cell **101:**635–645.
11. **Giaever, G., A. M. Chu, L. Ni, C. Connelly, L. Riles, S. Veronneau, S. Dow, A. Lucau-Danila, K. Anderson, B. Andre, A. P. Arkin, A. Astromoff, M. El-Bakkoury, R. Bangham, R. Benito, S. Brachat, S. Campanaro, M. Curtiss, K. Davis, A. Deutschbauer, K. D. Entian, P. Flaherty, F. Foury, D. J. Garfinkel, M. Gerstein, D. Gotte, U. Guldener, J. H. Hegemann, S. Hempel, Z. Herman, D. F. Jaramillo, D. E. Kelly, S. L. Kelly, P. Kotter, D. LaBonte, D. C. Lamb, N. Lan, H. Liang, H. Liao, L. Liu, C. Luo, M. Lussier, R. Mao, P. Menard, S. L. Ooi, J. L. Revuelta, C. J. Roberts, M. Rose, P. Ross-Macdonald, B. Scherens, G. Schimmack, B. Shafer, D. D. Shoemaker, S. Sookhai-Mahadeo, R. K. Storms, J. N. Strathern, G. Valle, M. Voet, G. Volckaert, C. Y. Wang, T. R. Ward, J. Wilhelmy, E. A. Winzeler, Y. Yang, G. Yen, E. Youngman, K. Yu, H. Bussey, J. D. Boeke, M. Snyder, P. Philippsen, R. W. Davis, and M. Johnston.** 2002. Functional profiling of the Saccharomyces cerevisiae genome. Nature **418:**387–391.
12. **Goode, S., M. Melnick, T. B. Chou, and N. Perrimon.** 1996. The neurogenic genes egghead and brainiac define a novel signaling pathway essential for epithelial morphogenesis during Drosophila oogenesis. Development **122:** 3863–3879.
13. **Goode, S., M. Morgan, Y. P. Liang, and A. P. Mahowald.** 1996. Brainiac encodes a novel, putative secreted protein that cooperates with Grk TGF alpha in the genesis of the follicular epithelium. Dev. Biol. **178:**35–50.
14. **Hamada, Y., Y. Kadokawa, M. Okabe, M. Ikawa, J. R. Coleman, and Y. Tsujimoto.** 1999. Mutation in ankyrin repeats of the mouse Notch2 gene induces early embryonic lethality. Development **126:**3415–3424.
15. **Hardy, K.** 1997. Cell death in the mammalian blastocyst. Mol. Hum. Reprod. **3:**919–925.
16. **Hendzel, M. J., Y. Wei, M. A. Mancini, A. Van Hooser, T. Ranalli, B. R. Brinkley, D. P. Bazett-Jones, and C. D. Allis.** 1997. Mitosis-specific phosphorylation of histone H3 initiates primarily within pericentromeric heterochromatin during G2 and spreads in an ordered fashion coincident with mitotic chromosome condensation. Chromosoma **106:**348–360.
17. **Hrabe de Angelis, M., J. McIntyre II, and A. Gossler.** 1997. Maintenance of somite borders in mice requires the Delta homologue DII1. Nature **386:**717–721.
18. **Jiang, R., Y. Lan, H. D. Chapman, C. Shawber, C. R. Norton, D. V. Serreze, G. Weinmaster, and T. Gridley.** 1998. Defects in limb, craniofacial, and thymic development in Jagged2 mutant mice. Genes Dev. **12:**1046–1057.
19. **Jurisicova, A., and B. M. Acton.** 2004. Deadly decisions: the role of genes regulating programmed cell death in human preimplantation embryo development. Reproduction **128:**281–291.
20. **Kamath, R. S., A. G. Fraser, Y. Dong, G. Poulin, R. Durbin, M. Gotta, A. Kanapin, N. Le Bot, S. Moreno, M. Sohrmann, D. P. Welchman, P. Zipperlen, and J. Ahringer.** 2003. Systematic functional analysis of the Caenorhabditis elegans genome using RNAi. Nature **421:**231–237.
21. **Krebs, L. T., Y. Xue, C. R. Norton, J. R. Shutter, M. Maguire, J. P. Sundberg, D. Gallahan, V. Closson, J. Kitajewski, R. Callahan, G. H. Smith, K. L. Stark, and T. Gridley.** 2000. Notch signaling is essential for vascular morphogenesis in mice. Genes Dev. **14:**1343–1352.
22. **Kress, C., S. Vandormael-Pournin, P. Baldacci, M. Cohen-Tannoudji, and C. Babinet.** 1998. Nonpermissiveness for mouse embryonic stem (ES) cell

derivation circumvented by a single backcross to 129/Sv strain: establishment of ES cell lines bearing the Omd conditional lethal mutation. Mamm. Genome **9:**998–1001.
23. **Kusumi, K., E. S. Sun, A. W. Kerrebrock, R. T. Bronson, D. C. Chi, M. S. Bulotsky, J. B. Spencer, B. W. Birren, W. N. Frankel, and E. S. Lander.** 1998. The mouse pudgy mutation disrupts Delta homologue Dll3 and initiation of early somite boundaries. Nat. Genet. **19:**274–278.
24. **Lai, E. C.** 2004. Notch signaling: control of cell communication and cell fate. Development **131:**965–973.
25. **Le Bras, S., M. Cohen-Tannoudji, V. Guyot, S. Vandormael-Pournin, F. Coumailleau, C. Babinet, and P. Baldacci.** 2002. Transcript map of the Ovum mutant (Om) locus: isolation by exon trapping of new candidate genes for the DDK syndrome. Gene **296:**75–86.
26. **Mitalipov, S. M., H. C. Kuo, J. D. Hennebold, and D. P. Wolf.** 2003. Oct-4 expression in pluripotent cells of the rhesus monkey. Biol. Reprod. **69:**1785–1792.
27. **Mumm, J. S., and R. Kopan.** 2000. Notch signaling: from the outside in. Dev. Biol. **228:**151–165.
28. **Nacerddine, K., F. Lehembre, M. Bhaumik, J. Artus, M. Cohen-Tannoudji, C. Babinet, P. P. Pandolfi, and A. Dejean.** 2005. The SUMO pathway is essential for nuclear integrity and chromosome segregation in mice. Dev. Cell. **9:**769–779.
29. **Nal, B., E. Mohr, M. I. Silva, R. Tagett, C. Navarro, P. Carroll, D. Depetris, C. Verthuy, B. R. Jordan, and P. Ferrier.** 2002. Wdr12, a mouse gene encoding a novel WD-repeat protein with a notchless-like amino-terminal domain. Genomics **79:**77–86.
30. **Nichols, J., B. Zevnik, K. Anastassiadis, H. Niwa, D. Klewe-Nebenius, I. Chambers, H. Scholer, and A. Smith.** 1998. Formation of pluripotent stem cells in the mammalian embryo depends on the POU transcription factor Oct4. Cell **95:**379–391.
31. **Niwa, H., Y. Toyooka, D. Shimosato, D. Strumpf, K. Takahashi, R. Yagi, and J. Rossant.** 2005. Interaction between Oct3/4 and Cdx2 determines trophectoderm differentiation. Cell **123:**917–929.
32. **Palmieri, S. L., W. Peter, H. Hess, and H. R. Scholer.** 1994. Oct-4 transcription factor is differentially expressed in the mouse embryo during establishment of the first two extraembryonic cell lineages involved in implantation. Dev. Biol. **166:**259–267.
33. **Pierce, G. B., A. L. Lewellyn, and R. E. Parchment.** 1989. Mechanism of programmed cell death in the blastocyst. Proc. Natl. Acad. Sci. USA **86:**3654–3658.
34. **Robertson, E. J., and A. Bradley.** 1986. Production of permanent cell lines from early embryos and their use in developmental problems, p. 475–508. *In* J. R. R. A. Pedersen (ed.), Experimental approaches to mammalian embryonic development. IRL Press, Oxford, United Kingdom.
35. **Rossant, J., and J. C. Cross.** 2001. Placental development: lessons from mouse mutants. Nat. Rev. Genet. **2:**538–548.
36. **Royet, J., T. Bouwmeester, and S. M. Cohen.** 1998. Notchless encodes a novel WD40-repeat-containing protein that modulates Notch signaling activity. EMBO J. **17:**7351–7360.
37. **Schweisguth, F.** 2004. Notch signaling activity. Curr. Biol. **14:**R129–R138.
37a. **Shi, S., M. Stahl, L. Lu, and P. Stanley.** 2005. Canonical notch signaling is dispensable for early cell fate specification in mammals. Mol. Cell. Biol. **25:**9503–9508.
38. **Sidow, A., M. S. Bulotsky, A. W. Kerrebrock, R. T. Bronson, M. J. Daly, M. P. Reeve, T. L. Hawkins, B. W. Birren, R. Jaenisch, and E. S. Lander.** 1997. Serrate2 is disrupted in the mouse limb-development mutant syndactylism. Nature **389:**722–725.
39. **Simmer, F., C. Moorman, A. M. van der Linden, E. Kuijk, P. V. van den Berghe, R. S. Kamath, A. G. Fraser, J. Ahringer, and R. H. Plasterk.** 2003. Genome-wide RNAi of C. elegans using the hypersensitive rrf-3 strain reveals novel gene functions. PLOS Biol. **1:**E12.
40. **Smith, T. F., C. Gaitatzes, K. Saxena, and E. J. Neer.** 1999. The WD repeat: a common architecture for diverse functions. Trends Biochem. Sci. **24:**181–185.
41. **Solter, D., and B. B. Knowles.** 1975. Immunosurgery of mouse blastocyst. Proc. Natl. Acad. Sci. USA **72:**5099–5102.
42. **Strumpf, D., C. A. Mao, Y. Yamanaka, A. Ralston, K. Chawengsaksophak, F. Beck, and J. Rossant.** 2005. Cdx2 is required for correct cell fate specification and differentiation of trophectoderm in the mouse blastocyst. Development **132:**2093–2102.
43. **Takai, H., K. Tominaga, N. Motoyama, Y. A. Minamishima, H. Nagahama, T. Tsukiyama, K. Ikeda, K. Nakayama, and M. Nakanishi.** 2000. Aberrant cell cycle checkpoint function and early embryonic death in Chk1(−/−) mice. Genes Dev. **14:**1439–1447.
44. **Tateishi, K., M. Omata, K. Tanaka, and T. Chiba.** 2001. The NEDD8 system is essential for cell cycle progression and morphogenetic pathway in mice. J. Cell Biol. **155:**571–579.
45. **Tomoda, K., N. Yoneda-Kato, A. Fukumoto, S. Yamanaka, and J. Y. Kato.** 2004. Multiple functions of Jab1 are required for early embryonic development and growth potential in mice. J. Biol. Chem. **279:**43013–43018.
46. **Vollrath, B., K. J. Fitzgerald, and P. Leder.** 2001. A murine homologue of the *Drosophila brainiac* gene shows homology to glycosyltransferases and is required for preimplantation development of the mouse. Mol. Cell. Biol. **21:**5688–5697.
47. **Voss, A. K., T. Thomas, P. Petrou, K. Anastassiadis, H. Scholer, and P. Gruss.** 2000. Taube nuss is a novel gene essential for the survival of pluripotent cells of early mouse embryos. Development **127:**5449–5461.
48. **Whittingham, D. G., and R. G. Wales.** 1969. Storage of two-cell mouse embryos in vitro. Aust. J. Biol. Sci. **22:**1065–1068.
49. **Xue, Y., X. Gao, C. E. Lindsell, C. R. Norton, B. Chang, C. Hicks, M. Gendron-Maguire, E. B. Rand, G. Weinmaster, and T. Gridley.** 1999. Embryonic lethality and vascular defects in mice lacking the Notch ligand Jagged1. Hum. Mol. Genet. **8:**723–730.
50. **Yagi, T., Y. Ikawa, K. Yoshida, Y. Shigetani, N. Takeda, I. Mabuchi, T. Yamamoto, and S. Aizawa.** 1990. Homologous recombination at c-fyn locus of mouse embryonic stem cells with use of diphtheria toxin A-fragment gene in negative selection. Proc. Natl. Acad. Sci. USA **87:**9918–9922.